# Kinetic Effects of an Unusually Large Neutral to Radical Cation Geometry Change. Slow Electron-Transfer Reactions between Alkylhydrazines

Stephen F. Nelsen,[*†] **Daniel T. Rumack,**[†] **and Michael Meot-Ner (Mautner)**[*‡]

Contribution from S. M. McElvain Laboratories of Organic Chemistry, University of Wisconsin, Madison, Wisconsin 53706, and Chemical Kinetics Division, Center for Chemical Physics, National Bureau of Standards, Gaithersburg, Maryland 20899. Received May 12, 1986

Abstract: High pressure mass spectrometry was used to measure the kinetics for electron transfer between 54 pairs of tetraalkylhydrazines containing acyclic and five- to seven-membered cyclic and bicyclic rings. Rate constants for electron transfer vary between 18 and 0.03×10^{-11} cm^3 molecule^{-1} s^{-1} at 550 K. Variable-temperature measurements were made on five pairs over a 77–120° range. The $(Me_2N)_2^+,(EtMeN)_2$ pair gave $E_a = 2.7$ kcal/mol. The association energy for $(Me_2N)_2$ was measured at $\Delta H° = -13.0$ kcal/mol near room temperature. These data are combined to estimate an energy separation of about 15.7 kcal/mol between associated $(Me_2N)_2^+/(EtMeN)_2$ dimer complex and the transition state for electron transfer. The observed Brønsted α value of about 0.5 suggests a large barrier to electron transfer, and the kinetics suggest that the components largely retain their original structures in the associated complex, but that significant distortion is required to reach the transition-state geometry. The effect of alkyl group changes on the electron-transfer rate and comparison of these data with solution experiments are discussed.

This work employed high-pressure mass spectrometry (HPMS) to a study electron-transfer reactions (eq 1). Vaporized mixtures

$$A^+ + B \underset{k_{-2}}{\overset{k_2}{\rightleftharpoons}} A + B^+ \qquad (1)$$
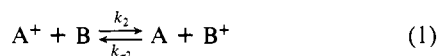
of an excess of benzene with small amounts of A and B (usually 0.1 to 5%) were subjected to an ionizing pulse. The benzene cation radicals initially formed rapidly generate a mixture of A^+ and B^+ initially close to the ratio of A/B present, but at the pressures employed (about 1 torr) electron transfer rapidly equilibrates A and B with their radical cations.

Success for studying electron transfer obviously requires that k_2 and k_{-2} be rapid relative to reactions decomposing the cation radicals. Although compounds with large π systems for delocalization of the odd electron in the cation radical typically allow equilibrium to be established, saturated compounds typically do not. The radical cations of most saturated compounds deprotonate too rapidly. We recently reported[1] that tetraalkylhydrazines (R_4N_2) do give long-lived radical cations under these conditions, allowing the electron-transfer equilibrium of eq 1 to be established. Examples of R_4N_2 provide particularly interesting cases for study, because in contrast to aromatic compounds, a significant geometry change accompanies electron loss. A great deal of work has established that unstrained neutral R_4N_2 examples have equilibrium geometries with their nitrogen atoms bent nearly tetrahedral, so the lone-pair orbitals have approximately sp^3 hybridization, and that there is a weak electronic preference for perpendicular lone pairs.[2] In contrast, unstrained $R_4N_2^+$ examples have nearly planar nitrogen atoms, so the lone pair orbitals have approximately pure p hybridization, and there is a strong electronic preference for coplanar lone pairs, because there are two bonding and one antibonding π electrons in the two-atom π system at nitrogen.[2c,3] Inclusion of rings between the alkyl substituents can substantially strain either of the oxidation states, making R_4N_2 electron-transfer equilbria extremely sensitive to what the alkyl groups attached to nitrogen are, despite the rather small electronic interaction of the alkyl groups with the lone pair electrons. Solution studies have shown very different characteristics for R_4N_2 electron transfers and those of compounds with large π systems, where little geometry change accompanies electron loss.[3] In this paper we discuss the rate constants associated with $R_4N_2, R_4N_2^+$ electron transfer in the gas phase. The related work on equilibrium constants will be published separately.

Results

The kinetics for electron transfer between 54 pairs of compounds were studied at 550 K. The kinetics for electron transfer were determined by following the ion intensities for 2–10 ms after the ionization pulse; the data obtained are summarized in Table I. Each entry has component A (eq 1) the harder to oxidize compound, so the reaction is exothermic in the forward direction, and k_2 is the faster rate constant for electron transfer. For facilitation of the discussion, Table I is broken into sections for which one component was a nonhydrazine reference compound (entries 1–3), both components were acyclic hydrazines (entries 4–18), at least one component was N,N-cycloalklyl (entries 19–35), and at least one component had an N,N'-cycloalkyl structure (entries 36–54). Within each section, the entries are arranged in order of decreasing exothermicity for the electron transfer, although the cases with branched alkyl groups present (entries 14–18) have been separated from the completely n-alkyl cases for the acyclic compounds. To avoid having to refer to a series of arbitrarily numbered structures to discover the components involved, the structures of the compounds are abbreviated in Table I, using besides the commonest alkyl group abbreviations, nPe for $CH_3(CH_2)_4$, neoPe for $(CH_3)_3CCH_2$, [r5N] for pyrrolidinyl, [r6N] for piperidinyl, [r7N]

[r5N]   [r6N]   [r7N]   (5)   (6)   (u6)

(7)   (221)   (222)   (330)
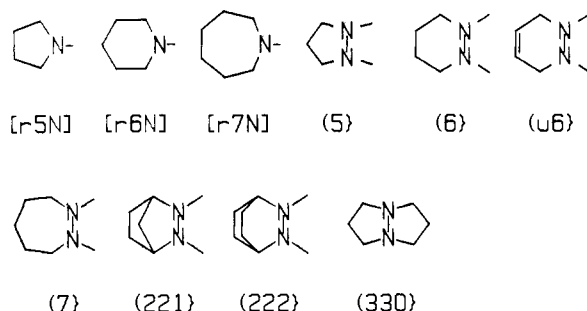
for homopiperidinyl, and the ones shown below for the N,N'-cycloalkyl compounds. Only k_2 is listed for the entries of Table I; k_{-2} is given by k_2/K_{eq}. In the units of Table I, [log (k_2) – log

---

(1) Meot-Ner (Mautner), M.; Nelsen, S. F.; Willi, M. R.; Frigo, T. B. *J. Am. Chem. Soc.* **1984**, *106*, 7384.

(2) (a) Shvo, Y. *The Chemistry of Hydrazo, azo, and Azoxy Groups*; Patal, S.; Ed.; Interscience: New York, 1975; Part 2, pp 1017–1095. (b) Nelsen, S. F. *Acc. Chem. Res.* **1978**, *11*, 14. (c) Nelsen, S. F. *Molecular Structures and Energetics*; Liebman, J. F., Greenberg, A., Eds.; VCH Publishers: Deerfield Beach, FL, 1986; Vol. 3, pp 1–86.

(3) Nelsen, S. F. *Acc. Chem. Res.* **1981**, *14*, 131.

[†] University of Wisconsin.
[‡] National Bureau of Standards.

Table I. Kinetic Data at 550 K for R_4N_2, $R_4N_2^+$ Electron Transfer

entry	component A	component B	ΔG°(550 K), kcal/mol	$k_2{}^a$	11 + log (k_c)
		Non-Hydrazine Reference Compounds			
1	azulene	$PhNMe_2$	−4.5	284	1.6
2	$PhNMe_2$	$TolNMe_2$	−4.7	145	1.2
3	$TolNMe_2$	$(Me_2N)_2$	−3.7	27	0.7
		Acyclic Hydrazines			
4	$(Me_2N)_2$	$(nPeMeN)_2$	−6.0	0.51	$(−1.5)^b$
5	$(Me_2N)_2$	$(nPrMeN)_2$	−4.6	0.28	−1.5
6	$(Me_2N)_2$	$(EtMeN)_2$	−3.0	0.22	−1.2
7	$(Me_2N)_2$	$nPeMeNNMe_2$	−3.0	0.18	−1.3
8	$nPeMeNNMe_2$	$(nPeMeN)_2$	−2.6	0.10	−1.5
9	$(Me_2N)_2$	$EtMeNNMe_2$	−1.7	0.15	−1.1
10	$(nPrMeN)_2$	$(nPeMeN)_2$	−1.7	0.03	−1.8
11	$EtMeNNMe_2$	$(EtMeN)_2$	−1.5	0.06	−1.5
12	$(EtMeN)_2$	$(nPrMeN)_2$	−1.5	0.03	−1.8
13	$(nPrMeN)_2$	$(nBuMeN)_2$	−1.2 {−1.5}	0.04	$−1.7^c$
14	$iBuMeNNMe_2$	$(nBuMeN)_2$	−3.4	0.11	−1.6
15	$(Me_2N)_2$	$iPrMeNNMe_2$	−3.1	0.20	−1.4
16	$(Me_2N)_2$	$iBuMeNNMe_2$	−2.2	0.08	−1.5
17	$(Me_2N)_2$	$(neoPeMeN)_2$	−1.7	0.04	−1.7
18	$EtMeNNMe_2$	$iPrMeNNMe_2$	−1.3	0.06	−1.5
		N,N-Cycloalkyl Hydrazines			
19	$(Me_2N)_2$	$[r5N]NMe_2$	−9.5	17.7	(−0.6)
20	$[r6N]NMe_2$	$[r5N]_2$	−6.5	4.3	(−0.6)
21	$[r7N]NMe_2$	$[r5NNr7]$	−1.8	0.05	−1.6
22	$[r5N]NMe_2$	$[r5N]_2$	−3.7	2.5	$−0.3^c$
23	$(nPeMN)_2$	$[r5N]_2$	−3.9	0.46	−1.1
24	$(Me_2N)_2$	$[r6N]NMe_2$	−2.9	0.55	−0.8
25	$[r6N]NMe_2$	$(nPeMeN)_2$	−2.8	0.16	−1.4
26	$[r6N]NMe_2$	$(nBuMeN)_2$	−2.6	0.20	−1.2
27	$[r6N]NMe_2$	$[r5N]NMe_2$	−2.4	0.50	−0.8
28	$[r6N]NMe_2$	$[r6N]_2$	−2.3	0.34	−0.9
29	$iPrMeNNMe_2$	$[r5N]NMe_2$	−2.3	0.29	−1.0
30	$[r6N]NMe_2$	$(iBuMeN)_2$	−2.3	0.10	−1.5
31	$[r6N]NMe_2$	$(neoPeMeN)_2$	−1.8	0.04	−1.7
32	$iBuMeNNMe_2$	$[r5N]NMe_2$	−1.8	0.05	−1.6
33	$[r5NNr6]$	$[r5NNr7]$	−4.6	0.79	−1.0
34	$[r6N]NMe_2$	$nPrMeN)_2$	−1.3	0.07	−1.4
35	$(nPrMeN)_2$	$[r6N]_2$	−1.2	0.08	−1.3
		N,N'-Cycloalkyl Hydrazines			
36	$(Me_2N)_2$	{222}	−10.4	18.2	(−0.8)
37	$(Me_2N)_2$	{6}	−4.8	4.0	(−0.3)
38	{6}	$[r5N]_2$	−4.6	3.6	(−0.3)
39	{u6}	$[r7N]NMe_2$	−3.4	1.29	−0.6
40	{16}	$(iBuMeN)_2$	−3.2	0.36	−1.6
41	{221}	{222}	−3.5	1.9	−0.4
42	{221}	$[r5N]_2$	−2.8 {−2.3}	1.6	$−0.3^c$
43	$(neoPeMeN)_2$	{5}	−2.7	0.15	−1.4
44	$(nPrMeN)_2$	{221}	−2.5	0.25	−1.1
45	{6}	{221}	−1.9	0.44	−0.7
46	$iPrMeNNMe_2$	{6}	−1.9	0.22	−1.0
47	$(neoPeMeN)_2$	{221}	−1.9	0.13	−1.3
48	$[r6N]NMe_2$	{5}	−1.9	0.50	−0.7
49	{7}	{330}	−1.9	1.26	−0.3
50	$[r6N]NMe_2$	{6}	−1.7	0.14	−1.2
51	$(EtMeN)_2$	{5}	−2.5	0.20	−1.0
52	$[r5N]NMe_2$	{221}	−1.4 {−1.7}	0.23	$−1.0^c$
53	$(iBuMeN)_2$	{221}	−1.4	0.09	−1.3
54	{u6}	$tBuMeNNMe_2$	−0.8	0.04	−1.5

^{a}Units are 10^{-11} cm^3 molecule^{-1} s^{-1}. ^{b}Numbers in parentheses are derived from k_{-2} values calculated from K_{eq}; k_{-2} was too small to affect the kinetic data. ^{c}Serious deviation between the number for ΔG° derived from K_{eq} obtained in the kinetic run, which is shown in braces, and that derived from a "tree" considering equilibria at several concentrations and for several compounds.

$(k_{-2})]/2\Delta G° = 0.197$. The data become less reliable when ΔG° is below about 1.5 kcal/mol, where the ion concentrations do not change upon approaching equilibrium, which limits the cases for which kinetic data were obtained to those with large enough ΔG°.

Results and Discussion: Activation Parameters for k_2

The most important thing to note about the rate data of Table I is the unusual size of the k_2 values. Exergonic gas-phase proton[4]

and electron-transfer[5-7] reactions typically have rate constants in the range of about 2×10^{-9} to 2×10^{-10} cm^3 molecule^{-1} s^{-1}; that is, they proceed with reaction efficiencies (ratio of observed rate constant to collision rate constant) in the range of 1 to 0.1. Much slower electron-transfer rates have been previously observed for electron exchanges in negative ion systems, between SF$_6$ and fluorinated alkanes.[8] Slow electron transfer has also been reported

(4) Su, T.; Bowers, M. T. *Int. J. Mass Spectrom. Ion. Phys.* **1973**, *12*, 347.

(5) Lias, S. G.; Ausloos, P.; Horvath, Z. *Int. J. Chem. Kinet.* **1976**, *8*, 725
(6) Meot-Ner (Mautner), M. *J. Phys. Chem.* **1980**, *84*, 2716.
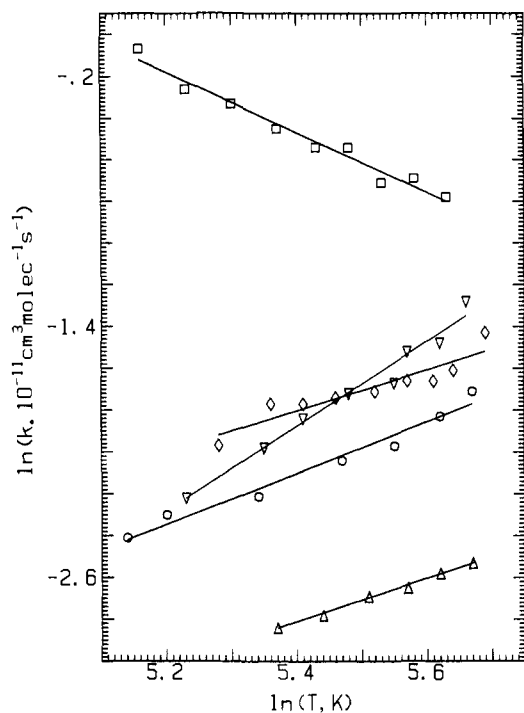(7) Meot-Ner (Mautner), M.; Sieck, L. W. *J. Phys. Chem.* **1982**, *86*, 3646.

Slow Electron-Transfer Reactions between Alkylhydrazines

J. Am. Chem. Soc., Vol. 109, No. 5, 1987 1375

Figure 1. Temperature dependence of rate constants: squares, entry 23; circles, entry 34; triangles; entry 6; inverted triangles, entry 44; diamonds, entry 52.

Table II. Activation Energies Calculated from Variable-Temperature Kinetic Data

entry[a]	compound pair	$E_a(k_2)^b$	$E_a(k_{-2})^b$	$\Delta G^{\circ a,b}$	$\Delta H^{\circ b,c}$
6	$(Me_2N)_2/(EtMeN)_2$	+2.7	+5.5	−3.0	−2.8
23	$(nPeMeN)_2/[r5N]_2$	−3.1	+2.7	−3.9	−5.5
34	$[r6N]NMe_2/(nPrMeN)_2$	+1.9	+4.5	−1.3	−2.5
44	$(nPeMeN)_2/\{221\}$	+4.4	+5.4	−2.5	−1.4
51	$(EtMeN)_2/\{5\}$	+2.1	+3.8	−2.5	−2.1

[a] Refers to Table I. [b] Units, kcal/mol. [c] Calculated from the temperature dependence of ΔG°. Such data will be presented in full in paper on equilibria of these reactions.
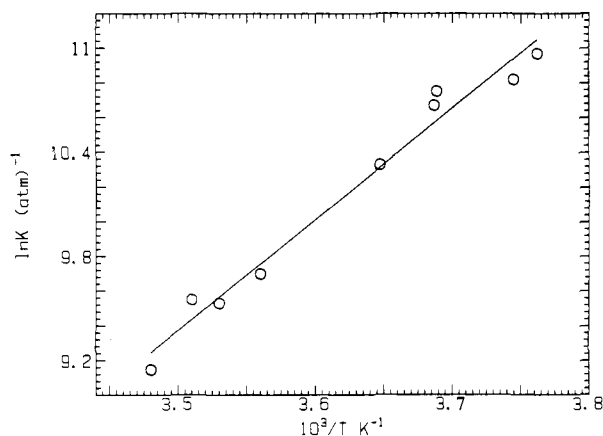

Figure 2. van't Hoff plot for the clustering reaction $Me_2NNMe_2^+$ + $Me_2NNMe_2 \rightarrow (Me_2NNMe_2)_2^+$.

by Eyler and Richardson for magnanocene and its cation, and attributed to an unusually large geometry change.[8d] As expected, the electron transfers involving aromatic compounds (entries 1 and 2) do proceed at fast rates, k_2 values of 2.8 and 1.4 × 10^{-9} being observed, but when one component was tetramethylhydrazine (entry 3), k_2 was only 0.1 times as large as for entry 1, and much slower rates were observed when both components of the pair were acyclic hydrazines. The k_2 values for entries 4–18 range from 1.8 × 10^{-3} to 1 × 10^{-4} times that of entry 1. The rates obviously increase as the reactions become more exothermic, but in the fastest of the acyclic hydrazine pairs only about one-thousandth of the collisions are reactive.

Temperature coefficients for slow ion–molecule reactions which have rates in the 10^{-13} to 10^{-11} cm³ molecule⁻¹ s⁻¹ range often show substantially negative temperature coefficients ($k = cT^{-n}$ with n between 3 and 10). Arrhenius activation energies as negative as −14 kcal/mol have been reported,[9] yet the rate constants are small because of small preexponential factors (negative $\Delta S^{\ddagger}$ values using transition-state theory). Gas-phase methyl-transfer reactions are examples of processes which have substantial energy barriers which combine with the small preexponential factors to give small negative or positive temperature coefficients, corresponding to E_a values of −4 to +4 kcal/mol.[10] In this work we succeeded in obtaining variable-temperature kinetic data for five of the compound pairs of Table I (over 77 to 120° temperature ranges centered from 225 to 252 °C) and present these data in Figure 1. Our measurements were made at 0.6 to 1.4 torr, with all reactants fully thermalized. The rate constants obtained are found to be pressure independent in this range. A ln k_2 vs. ln T plot of these data appears as Figure 1, and the Arrhenius activation energies calculated are shown in Table II, along with ΔG° values at 550 K (277 °C) from Table I and ΔH° values calculated from the temperature dependence of ΔG°. It may be noted that the most exothermic reaction, entry 22, gave a negative $E_a(k_2)$ value,

but the others observed were small and positive. Also note that there is a rough trend toward higher E_a values for the reactions with less negative ΔH° values, with entry 44, which has the least negative ΔH°, having the most positive $E_a(k_2)$. The activation energies of Table II are quite similar to those found for methyl-transfer reactions by the groups of Kebarle and of Brauman.[10]

Discussion

1. Potential Energy Surfaces. We attribute the small rate constants and often positive activation energies for hydrazine electron-transfer reactions to substantial barriers for electron transfer, because of the well-documented large geometry change which accompanies electron loss from hydrazines. Seeing even small positive activation energies implies large barriers for the electron transfer, because ions stick rather tightly to neutral molecules in the gas phase, where solvent is not available for charge delocalization. An associated dimer radical cation complex, which we shall refer to as $A^+ \cdot B$, is an intermediate in gas-phase electron-transfer reactions. Measurements on tetramethylhydrazine at much lower temperatures than those used for the electron-transfer rate measurements allowed observation of the $(Me_2N)_2/(Me_2N)_2^+$ dimer radical cation, and the variable-temperature data of Figure 2 gave a ΔH° of association of −13.0 kcal/mol, and ΔS° of association of −26.8 cal/mol·K. Similar measurements on hydrazines with larger alkyl groups were not made, so we cannot quantitatively address the question of how alkyl group changes affect the association energy. We suggest that similar association energies are likely to be involved for all of the hydrazine pairs which contain only n-alkyl groups, and that entry 6 is likely to have an association energy closest to the measured value of the cases studied. Our data then, produce the energy profile for the entry 6 case which is shown in Figure 3. The barrier for electron transfer within the associated dimer radical cation is estimated at about 15.7 kcal/mol starting from the $(Me_2N)_2^+/(EtMeN)_2$ complex $A^+ \cdot B$, to reach the electron-transfer state, $(A \cdot B)^{+\ddagger}$. Marcus theory[11] assumes that the transition state for electron transfer has the reactants distorted to geometries

(8) (a) Fehsenfeld, F. C. *J. Chem. Phys.* **1971**, *54*, 438. (b) Streit, G. E. *Ibid.* **1982**, *77*, 826. (c) Grimsrud, E. P.; Caldwell, G.; Chawdhury, S.; Kebarle, P. *J. Am. Chem. Soc.* **1985**, *107*, 4267. (d) Eyler, J. R.; Richardson, D. E. *Ibid.* **1985**, *170*, 6130.

(9) Meot-Ner (Mautner), M.; Field, F. H. *J. Am. Chem. Soc.* **1978**, *100*, 1356.

(10) (a) San Sharma, D. K.; Kebarle, P. O. *J. Am. Chem. Soc.* **1982**, *102*, 19. (b) Dodd, J. A.; Brauman, J. I. *Ibid.* **1984**, *106*, 5356.

(11) (a) Marcus, R. A. *Annu. Rev. Phys. Chem.* **1964**, *15*, 155. (b) Marcus, R A. *Special Topic in Electrochemistry*; Rock, P. A., Ed.; Elsevier: Amsterdam, 1977; p 161. (c) Eberson, L. *Adv. Phys. Org. Chem.* **1982**, *18*, 79–185.
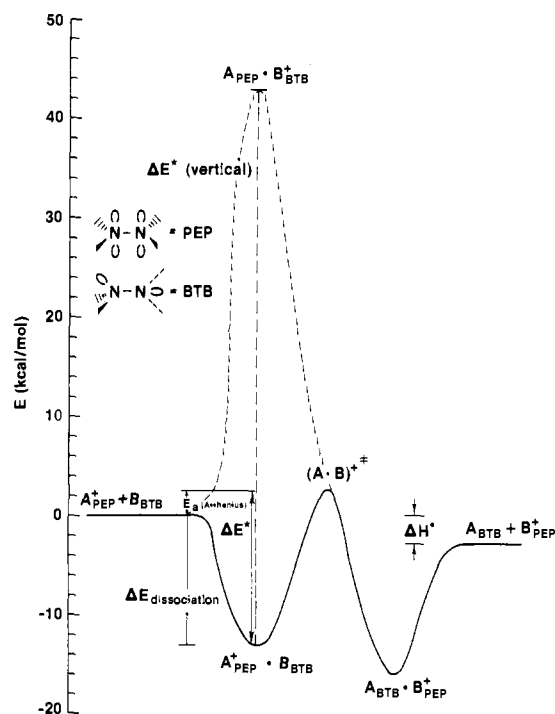
Figure 3. Energy diagram for electron transfer between $(Me_2N)_2^+$ and $EtMeN)_2$ (entry 6 of Table I). The numbers are in kcal/mol. See ref 1 for a discussion of the perpendicular–eclipsed-perpendicular and beni–twisted-beni (PEP and BTB) designations used to label the curves.

Figure 4. Correlation between ln (k_2) $(10^{-11}$ cm^3 s$^{-1})$ and $\Delta G°$ (kcal/mol) for reactions of acyclic (circles) and cyclic (squares) tetraalkyl-hydrazines.

intermediate between those of the neutral and cation equilibrium structures, which leads to a barrier one-quarter the size of that for vertical electron transfer to give the neutral species in the cation geometry and the cation in the neutral species geometry. For the hydrazine electron transfers, the relaxation energies of the cation radicals, numerically the difference between the vertical and adiabatic ionization potentials, (vIP – aIP), are not only unusually large, but have been measured. Figure 3 shows a comparison of the estimated vertical electron-transfer barrier with the observed barrier; the internal geometry changes (the "inner shell" term in Marcus theory) lower the barrier to electron transfer on the order of 40 kcal/mol for acyclic hydrazines.

An Arrhenius treatment of the rate data is clearly invalid and does not yield a realistic activation energy when the electron-transfer rate decreases as the temperature is increased (such as Table II, Entry 23). Here the energy change from the reactants to the activated complex is negative, and the energy distribution for the reacting complexes is not Boltzman. For the cases with an increase in activation energy as temperature is increased, however, the Arrhenius treatment provides a significant comparison with rates measured in solution.

2. Relation between Rate and Exoergocity. The rate constants of Table I obviously increase as the reactions become more exothermic. More quantiatively, Figure 4 shows the relation between ln k_2 and $\Delta G°$ for selected pairs. We plot only reactions for which $\Delta G° < -2$ kcal/mol because the data are less accurate for less exoergonic reactions, and because other factors can become dominant. Figure 4 shows that acyclic structures and pairs containing at least one ring give data lying close to different lines. For the cyclic cases (squares), only cases with the noncyclic substituents being methyl groups have been plotted. Larger alkyl groups have an additional rate-slowing effect, as will be discussed below. For a given $\Delta G°$, the cyclic cases are faster than the acyclic cares by a factor of about 5. Similar trends have been observed in charge-transfer reactions of alkanes and in hydride-transfer reactions between carbonium ions, and have been interpreted on the basis of steric effects.[9,12] In terms of transition-state theory,
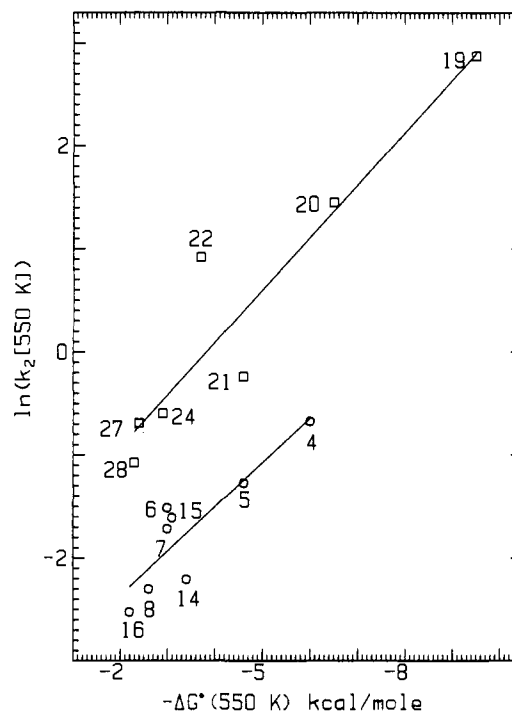
the rate-slowing effects of the acyclic substituents were associated with an entropy loss of the transition state because the rotational freedom of the alkyl groups becomes restricted.

Linear regression analysis yields the Brønsted slope $\alpha = d\Delta G^*/d\Delta G° = RT$d ln $k_2/d\Delta G° = 0.48 \pm 0.1$ (correlation coefficient 0.87) for the acyclic cases, and 0.56 ± 0.1 (correlation coefficient 0.94) for the cyclic cases of Figure 4. The expected α values can be calculated independently from the Marcus equations:

$$\Delta G^* = ((\Delta G°)\ 2/16\Delta G_0^*) + \Delta G_0^* + \tfrac{1}{2}[\Delta G°]^2 \quad (2)$$

$$\alpha = d\Delta G^*/d\Delta G° = \tfrac{1}{2} + (\Delta G°/8\Delta G_0^*) \quad (3)$$

Following the practice of Dodd and Brauman,[10b] potential energies (or here, enthalpies) are substituted for free energies. Referring to Figure 3, the $\Delta H°$ to use is the difference between the bottoms of the two wells A^+B and B^+A. Since the binding energies of the two complexes should be very similar, we use $\Delta H° = \Delta H(\text{rxn}) = -2.8$ kcal/mol, which also follows Dodd and Brauman. From Figures 3, $\Delta G^* = 15.7$ kcal/mol, so eq 2 gives $\Delta H°^* = 17.1$ kcal/mol for the intrinsic barrier, and eq 3 an α value of 0.48, which agrees well with the value arrived at by comparing examples with various n-alkyl substituents. In fact, eq 2 shows that α will be near 0.5 whenever the intrinsic barrier is significantly larger than the exothermicity, which is certainly true for these hydrazines.

3. Effect of Alkyl Group Changes on Electron-Transfer Rate. We shall now consider how changes in the alkyl groups of the two components affect the rate of electron transfer in more detail. As pointed out in the previous section, the size of k_2 clearly depends on the exothermicity of the reaction. To eliminate the $\Delta G°$ effect, we shall consider the "intrinsic" electron-transfer rate constants log (k_e), as defined in eq 4. k_e is effectively adjusted to $\Delta G° =$

$$\log (k_e) = [\log (k_2) + \log (k_{-2})]/2 \quad (4)$$

0, and is exactly equivalent to extrapolating each point in a log (k) vs. $\Delta G°$ (Marcus) plot to $\Delta G° = 0$. Eberson discusses the generality of such a Marcus treatment in his review of electron transfer in organic compounds.[11c] Even our fastest measured rates for hydrazine pairs (entries 19 and 36 of Table I) are only on the order of 6% of the collison rate, so our data should mostly be out of the region of curvature in a Marcus plot. We suggest that the

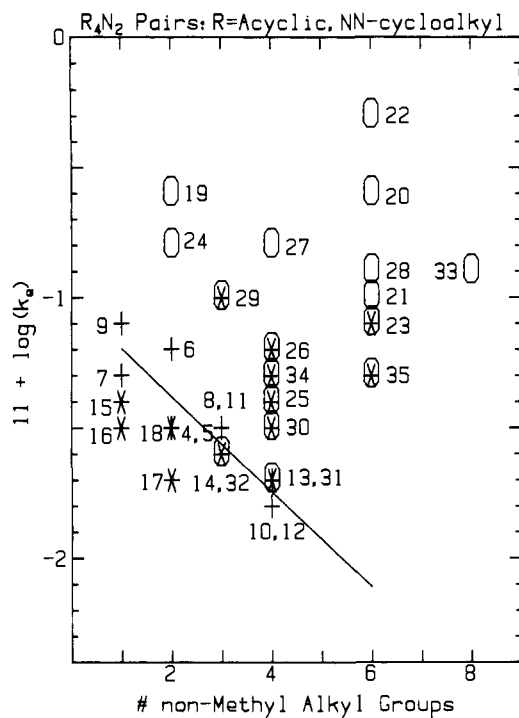(12) Meot-Ner (Mautner), M.; Sieck, L. W. *J. Am. Chem. Soc.* **1983**, *105*, 2986.

Figure 5. Plot of 11 + log (ke) vs. # of nonmethyl alkyl groups for tetraalkylhydrazine pairs: methyl and n-alkyl compounds (entry 4–13), +; acyclic branched alkyl compounds (entries 14–18), *; N,N-cycloalkyl methyl compounds, open ovals; N,N-cycloalkyl nonmethyl alkyl compounds, filled ovals.

Figure 6. Plot of 11 + log (k_e) vs. # of nonmethyl alkyl groups for pairs which include N,N'-cycloalkyl groups. The filled symbols are for pairs which include nonmethyl acyclic alkyl groups. The numbers identify the pairs involved (Table I).

advantage of this treatment is that log (k_e) values may be directly compared and the differences between the numbers attributed to structural differences in the hydrazines involved. The overall reproducibility of the 11 + log (k_e) values (last column of Table I) appears to be on the order of 0.1 to 0.2 units, from internal comparison of the data for closely related compounds pairs.

The values observed for the 10 pairs in which all R groups are methyl or n-alkyl (entries 4–13) make it clear that lengthening the alkyl groups in both A and B components of eq 1 decreases the rate of electron transfer; the decrease is approximately additive as methyl groups are replaced by n-alkyl groups. The crosses in Figure 5 are a plot of 11 + log (ke) vs. the number of alkyl groups larger than methyl on both components (#, which can in principle be up to 8, although only one # = 8 pair was run, entry 33). The pairs with one and two ethyl groups (entries 9 and 6, respectively) show marginally faster rates than those with longer alkyl groups, but this may only be experimental error, and no significant differences between nPr, nBu, and nPe groups was observed. Ion-molecule clustering data, as for the dimer ions of nPr_3N and nBu_3N, show that going from n-propyl to n-butyl substituents does not necessarily increase the entropy loss significantly.[13] This occurs because the outer alkyl group portions do not lose much rotational freedom in the complex. The least-squares line through the methyl, n-alkyl compounds (crosses) is reasonably straight (correlation coefficients 0.90, average deviation 0.09 log unit, maximum deviation 0.16 log unit), 11 + log (k_e) = −1.016 − 0.182(#). Runs for the five acyclic pairs which include branched alkyl groups, entries 14–18, asterisks in Figure 5, show slightly smaller k_e values than n-alkyl pairs of the same # value. On the basis of these very limited data, we cannot distinguish between the sizes of the additional rate decrease for the α-branched isopropyl and the β-branched isobutyl and neopentyl groups, which appear to lie between 0.1 and 0.2 log unit per branched alkyl group. Runs for the 17 pairs which include N,N-cycloalkyl groups (entries 19–35) are shown as ovals in Figure 5. The unfilled symbols are for cases in which only N,N-cycloalkyl groups and methyl groups are present, and the plot shows that the k_e-lowering factor when
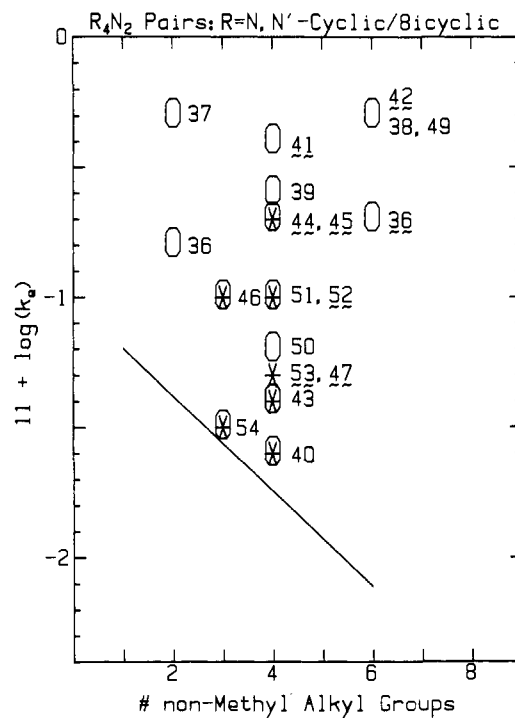
methyl is replaced by n-alkyl disappears when the normal alkyl groups are linked into N,N-cycloalkyl rings. This is consistent with the rotational restriction mentioned in the previous section being important. The filled symbols include cases with both n-alkyl and branched alkyl groups, and examination of the plot demonstrates that the presence of n-alkyl groups still lowers k_e when N,N-cycloalkyl groups are also present, and that branched alkyl groups still lower k_e more than do n-alkyl groups. Two neopentyl groups (entry 31) or one $tert$-butyl group (entry 32) cancel the increase in k_e caused by the presence of a cycloalkyl R_2N group. Considering only the cases with methyl and n-alkyl groups and one type of R_2N group, deviations from the n-alkyl line suggest that the pyrrolidinyl group [r5N] causes a larger k_e increase than does the piperidinyl group [r6N]; entries 19, 22, 23, and 29 average to a +0.61 log unit increase per [r5N] group, while entries 24–26, 28, 34, and 35 average to a +0.45 increase per [r6N] group. A smaller increase is probably caused by the homopiperidinyl group [r7N], but only two pairs, entries 21 and 33, have this group, and both also have at least one other cycloalkyl group, so the size cannot be estimated well.

The k_e data for the 19 N,N'-cycloalkyl cases examined (entries 36–54 of Table I) are plotted in the same way in Figure 6. Once again, the open symbols show cases with only cycloalkyl and methyl substituents, and the filled symbols include larger acyclic substituents. Two β-branched alkyl substituents (entries 40, 43, 46, and 51) or one $tert$-butyl substituent (entry 54) mostly cancel the k_e increase caused by N,N'-cycloalkyl substituents. The bond rotation restriction argument used for the N,N-cycloalkyl substituents is also applicable for N,N'-cycloalkyl groups, and doubtless causes part of the k_e increase observed, but we note that large deviations from additivity of the effects are present especially for the hexahydropyridazinyl group {6}, because entry 37, which pairs {6} with tetramethylhydrazine has an 11 + log (k_e) value 0.9 log unit higher than entry 50, in which {6} is paired with [r6N]NMe$_2$, although the latter hydrazine itself shows a substantial rate increase when paired with n-alkyl compounds. The entry numbers of pairs including the N,N'-bicycloalkyl compounds {221} and {222} are underlined in Figure 6, and examination of the plot shows another large effect on k_e. Throughout our data, branching of the alkyl groups leads to significant rate decreases

(13) Meot-Ner, M.; Field, F. H. *J. Chem. Phys.* **1976**, *64*, 277.

when two branched alkyl groups appear in the same hydrazine. Although the α carbons of the {221} and {222} hydrazines are secondary, the bicyclic rings force their CN bonds to be rotated to maximize steric interactions with an approaching molecule, and one might have anticipated that these compounds would have shown large rate decreases because of their great steric hindrance. Instead, the 11 + log (k_e) values observed for the bicyclic hydrazines are comparable to those for unbranched N,N'-cycloalkyl groups.

Several different effects are clearly responsible for the distribution of log (k_e) values shown in Figures 5 and 6. Referring to Figure 3, decreases in rate could be caused either by an increase in the $(A \cdot B)^{+\ddagger}, A^+ \cdot B$ energy gap as branching increases, or by raising the energy of the complex $A^+ \cdot B$ as the alkyl groups are enlarged, without significantly affecting the energy gap. Both would raise the energy of the transition state relative to the free molecules. Entropy factors associated with increased hindrance of a larger number of free rotors could also be involved. We are unable to presently address the relative importance of these effects; what we observe is their sum.

The N,N'-cyclic alkyl groups force the NN bond to assume electronically unfavorable conformations with the lone-pair, lone-pair dihedral angle θ significantly different from the 90° found for acyclic compounds and the N,N-cycloalkyl compounds discussed here. We suggest that the structural changes involved with this NN rotational change may well be involved in the rate increases observed in the gas phase for N,N'-cycloalkyl hydrazines. Heterogeneous electron-transfer rate constants in solution have been shown to be higher when θ is 180° than when it is near 60°, providing a solution analogy for such an effect.[2b] The reason for {6} showing such great variability in its effect on electron-transfer rate depending on its partner probably has something to do with the presence of the diequatorial $\theta = 180°$ and axial, equatorial $\theta = 60°$ conformations of similar energy but with different steric requirements;[2] we are unable to say what is involved in detail yet, however. Large enough deviations from additivity to be obvious in these rate data were also observed for other N,N'-cycloalkyl hydrazines.

4. Structure of $A^+ \cdot B$ and $(A \cdot B)^{+\ddagger}$. The structural features of the associated dimer radical-cation ground state, $A^+ \cdot B$, and of the transition state for electron transfer, $(A \cdot B)^{+\ddagger}$, are of obvious interest. Although the HPMS technique requires that A and B of eq 1 be different compounds, it is easier to think about "homogeneous" electron transfers, in which A and B are the same, and $\Delta G°$ is zero, and we shall use a homogeneous electron transfer involving hydrazines as the basis of this discussion. Marcus theory for electron transfer[11] uses the fact that electrons are far lighter than nuclei to argue that the electron transfer itself will be instantaneous once the electron-transfer transition state has been reached. The observed barrier to electron transfer corresponds to the energy required to distort the structures of the neutral and oxidized components until they reach the same geometry, that of the transition state. $(A \cdot B)^{+\ddagger}$ ought to have an axis or plane of symmetry because the two components have the same geometry. This work provides the experimental estimate that $(A \cdot B)^{+\ddagger}$ lies about 15.7 kcal/mol higher in energy than does $A^+ \cdot B$ for the $(Me_2N)_2/(EtMeN)_2$ (entry 6) case. This implies that the cationic and neutral components of $A^+ \cdot B$ are likely to have very different structures, to allow their energy to be very different from when they have similar structures, in $(A \cdot B)^{+\ddagger}$. The structures of isolated cationic and neutral hydrazines are, of course, very different. The slow electron transfer observed implies to us that their geometries cannot have become similar in $A^+ \cdot B$.

For trialkylamines, there is conclusive evidence in the work of Alder and co-workers[14] that R_3N^+/R_3N pairs form associated radical-cation dimer complexes which adopt a symmetrical structure with the odd electron in the σ^* orbital of an NN bond, corresponding to I. These species are even isolable in cases where

I   II
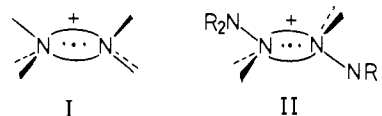
the nitrogens are bridged with three $(CH_2)_3$ or $(CH_2)_4$ groups.[15] The strength of the NN 3e-σ bond has been estimated at about 15 kcal/mol by two very different experiments.[16] The analogous structure for a hydrazine would be the 3e-σ bonded species II. We point out that II is not an energy minimum, however. Solution studies on complex polycyclic bishydrazines in which the rings encourage approach of the hydrazine units give no evidence that II formation is thermodynamically favorable,[17] indirect contrast to the diamine cases studied by Alder. Our conclusion from this work[17] was that N,N'-bisamino substitution of I, as in II, greatly destabilizes the 3e-σ bond. This seems entirely reasonable on independent grounds. Going from an isolated hydrazine radical cation and a neutral hydrazine to II requires loss of the resonance stabilization of the 3e-π bond of the hydrazine radical cation, and gains the stabilization of the 3e-σ bond. The strength of the 3e-π bond of a tetraalkylhydrazine radical cation has been measured at over 20 kcal/mol from the rotational barrier observed for 8,8'-bi(8-azabicyclo[3.2.1]octane) (**55**) cation radical, and an ab initio calculation (MP2-6-31-G* level) of the rotational barrier for the parent $H_4N_2^+$ gave 30.2 kcal/mol.[18] Unless the 3e-σ bond of II were substantially stronger than that of I, formation of II from the relaxed cation and neutral species ought to cost energy, not lead to stabilization as it does the amine case. The results of molecular orbital calculations agreeing with these statements will be published elsewhere.

5. Gas- and Solution-Phase Hydrazine Electron Transfer. Solution-phase rate constants for tetraalkylhydrazine electron-transfer reactions have recently become available, allowing comparison of these reactions in the two phases. Rate constants for electron transfer between **55**$^+$ and **55** have been measured by cyclic

55   56
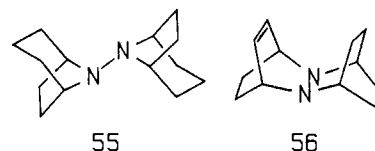
voltammetry and by UV spectroscopy, giving consistent results.[18] Because the cation radical exists in two isomers which differ in energy by 1.5 kcal/mol, we extrapolated the rate constants to $\Delta G° = 0$ in the same way as we did for the gas-phase k_e values, obtaining k_e(22 °C) = 1.1 × 10^3 M^{-1} s^{-1}, corresponding to ΔG^*_e = 13.1 kcal/mol in CH_3CN solution containing 0.15 M tetra-n-butylammonium perchlorate. The bicyclic alkyl groups of **55** enforce anti geometries (θ = 180°) in both oxidation states.[18] "Self"-electron-transfer rates between the syn bent (θ = 0°) hydrazine **56** and its radical cation may be measured especially accurately because electron transfer is rapid enough to allow the use of NMR line broadening, and the amount of line broadening for the vinyl ^{1}H NMR signal may be accurately measured. In CD_2Cl_2 solution, **56**$^+$-NO$_3^-$/**56** shows k_e(23 °C) of 5.4 × 10^4 M^{-1} s^{-1}, corresponding to ΔG^*_e = 10.9 kcal/mol, and activation parameters of ΔH^*_e = 7.4 kcal/mol and ΔS^*_e = -12 cal/mol deg were determined.[19] The alkyl groups of both **55** and **56** force them to assume electronically destabilized conformations with

(14) For a review, see: Alder, R. W.; Sessions, R. B. *Chemistry of Amino, Nitrogen, and Nitro Compounds and Their Derivatives*; Patai, S., Ed.; Wiley: New York, 1982; Part 2, chapter 18, p 762.

(15) (a) Alder, R. W.; Sessions, R. B.; Mellor, J. M.; Rawlins, M. F. *J. Chem. Soc., Chem. Commun.* **1977**, 747. (b) Alder, R. W.; Sessions, R. B. *J. Am. Chem. Soc.* **1979**, *101*, 3652. (c) Alder, R. W.; Orpen, A. G.; Sessions, R. B. *J. Chem. Soc., Chem. Commun.* **1985**, 949.

(16) (a) Nelsen, S. F.; Alder D. W.; Sessions, R., B.; Asmus, K.-D.; Hiller, K.-O.; Göbl, M. *J. Am. Chem. Soc.* **1980**, *102*, 702. (b) Alder, R. W.; Arrowsmith, R. J.; Casson, A.; Sessions, R. B.; Heilbronner, E.; Kovac, B.; Huber, H.; Taagepera, M. *Ibid.* **1981**, *103*, 6137.

(17) Nelsen, S. F.; Willi, M. R.; Mellor, J. M.; Smith, N. M. *J. Org. Chem.* **1986**, *51*, 2081.

(18) Nelsen, S. F.; Cunkle, G. T.; Evans, D. H.; Haller, K. J.; Kaftory, M.; Kirste, B.; Kurreck, H.; Clark, T. *J. Am. Chem. Soc.* **1985**, *107*, 3829.

(19) Nelsen, S. F.; Blackstock, S. C. *J. Am. Chem. Soc.* **1985**, *107*, 7189.

coplanar lone pairs and strain the neutral compounds more than the radical cations, as indicated by the low solution oxidation potentials for these species (their formal oxidation potentials in solution correspond to 4.6 and 15.2 kcal/mol easier oxidation than for $EtMeN)2$). Large geometry changes between neutral and radical cationic forms do occurr for both species, the NN bonds shortening by about 10%, and the nitrogens flattening significantly, as shown by X-ray crystallography.[18,20] Associated radical-cation dimers may very well be intermediates in solution as well as in the gas-phase electron transfer, but because solvation is present for the radical cation in solution, we do not expect large binding energies for such species, and believe that the solution barriers observed ought to correspond closely to the $A^+ \cdot B, (A \cdot B)^{+\ddagger}$ energy gap in solution. Although there are obviously differences between gas-phase and solution reactions, we find the similarity in barrier heights and somewhat higher gas-phase for entry 6 than for the unquestionably more strained solution cases to be quite striking. These results are quite consistent with the principal cause of slow electron transfer between hydrazines and their cations being the large geometry change entailed; this geometry change is independent of phase.

Summary

Electron-transfer reactions between hydrazines constitute a rare series of slow electron-transfer reactions in organic systems in the gas phase. The main trends observed are: slow rates, correlation of k with $\Delta G°$, small positive or negative activation energies, and increased rates of cyclic compared to acyclic reactants. In all these respects, slow electron-transfer reactions resemble slow heavy particle (H^-, CH_3^+) transfer reactions. The low efficiencies observed are associated with substantial barriers due to the large geometry change required to proceed from the associated reactant pair $A^+ \cdot B$ to the transition state $(A \cdot B)^{+\ddagger}$. The slow observed rate constant, positive activation energy, and Brønsted slope near 0.5 all suggest a large "inner sphere" term in Marcus theory. Knowledge of the $A^+ \cdot B$ association energy, the Arrhenius activation energy, and hydrazine cation relaxation energies allow the construction of a full potential energy surface. Effects of the hydrazine lone-pair distortions are noted, especially in increasing the rates for bicyclic hydrazines. Possible entropy effects are also noted in lowering the rates with increasing alkyl substitution.

Experimental Section

Compounds Employed. The hydrazines were synthesized by reductive alkylation of di- or trimethylhydrazine,[21] or by other previously described methods.[22] Proton NMR spectra in $CDCl_3$ are reported below in δ units for compounds previously not described.

n-Pentyltrimethylhydrazine: 0.9 (m, 3 H), 1.3 (m, 4 H), 1.6 (m, 2 H), 2.2 (s, 3 H), 2.3 (s, 6 H), 2.4 (t, 2 H).

1,2-Di-*n*-propylhydrazine: 0.9 (t, 6 H), 1.5 (m, 4 H), 2.2 (s, 6 H), 2.4 (t, 6 H).

1,2-Di-*n*-butyldimethylhydrazine: 0.9 (t, 6 H), 1.4 (m, 8 H), 2.2 (s, 6 H), 2.4 (t, 4 H).

1,2-Di-*n*-pentylhydrazine: 0.9 (t, 6 H), 1.2–1.5 (m, 12 H), 2.2 (s, 6 H), 2.4 (t, 4 H).

HPMS Experiments. Measurements were carried out on the NBS pulsed high-pressure mass spectrometer, which has been previously described.[23] The general procedure for acquiring kinetic data is as follows. Samples of the two compounds to be compared were injected into a heated (150 °C) bulb along with 400 μL of benzene (600 μL for variable-temperature experiments) and 50 μL of chloroform-saturated air. The needle valve connecting the bulb with the ionizing chamber was opened, and the flow was adjusted until the pressure in the chamber was ~1.6 torr. Dialing to a mass corresponding to one of the species revealed a counts vs. time profile (approx. 30 ms in duration). It is this profil that was acquired. To account for fluctuations in temperature and pressure, 512 scans of mass 1, followed by 1024 scans of mass 2, and finally, 512 scans of mass 1 were obtained. The ratios of the two ions vs. time were printed, and a calculation of the equilibrium constant was performed on a segment corresponding to equilibrium (constant ion ratio). This equilibrium constant was then used in the kinetic calculations. The kinetics of electron transfer were acquired by running the kinetics program on a section of the time profile prior to equilibrium, using the standard equations for reversible bimolecular kinetics. The time profile used in this experiment was created by a pulsed, ionizing filament. The chamber was exposed to the filament for ~1–2 ms, with a delay of ~30 ms, which could be varied from experiment to experiment. This pulse ionized everything in the chamber approximately in proportion to the fraction of its neutral form, generating mostly $C_6H_6^+$ ions from the carrier gas. These reacted rapidly to generate the $R_2NNR_2^+$ cation radicals, which then reacted during the pulse delay time, bringing the mixture to equilibrium. During this time, the ions diffused out of the chamber through a mass detector, where the ions of chosen mass were selected, multiplied, and counted. The count vs. time relative to pulse initiation were then displayed on an oscilloscope and manipulated as described above.

(20) Nelsen, S. F.; Blackstock, S. C.; Haller, K. J. *Tetrahedron* **1986**, *42*, 6101.

(21) Nelsen, S. F.; Peackock, V.; Weisman, G. R. *J. Am. Chem. Soc.* **1976**, *98*, 5269.

(22) Nelsen, S. F.; Hintz, J. *J. Am. Chem. Soc.* **1972**, *94*, 7108.

(23) Meot-Ner (Mautner), M.; Sieck, L. W. *J. Am. Chem. Soc.* **1983**, *105*, 2956.